On the Numerical Solution of Widely Used 2D Stochastic Partial Differential Equation in Representing Reaction-Diffusion Processes

Nasrin Samadyar[1,2] (ID) and Yadollah Ordokhani[1*] (ID)

[1]Department of Mathematics, Faculty of Mathematical Sciences, Alzahra University, Tehran, Iran
[2]Department of Basic Science, Kermanshah University of Technology, Kermanshah, Iran

Abstract

In this paper, a combined methodology based on the method of lines (MOL) and spline is implemented to simulate the solution of a two-dimensional (2D) stochastic fractional telegraph equation with Caputo fractional derivatives of order α and β where $1 < \alpha, \beta \le 2$. In this approach, the spatial directions are discretized by selecting some equidistance mesh points. Then fractional derivatives are estimated via linear spline approximation and some finite difference formulas. After substituting these estimations in the semi-discretization equation, the considered problem is transformed into a system of second-order initial value problems (IVPs), which is solved by using an ordinary differential equations (ODEs) solver technique in Matlab software. Also, it is proved that the rate of convergence is $O(\Delta x^2 + \Delta y^2)$, where Δx and Δy denote the spatial step size in x and y directions, respectively. Finally, two examples are included to confirm the efficiency of the suggested method.

1 Introduction

Partial differential equations (PDEs) due to their connection with real phenomena are one of the most extensive topics in mathematical researches. PDEs play a crucial role in modeling various phenomena in chemistry. They form the basis for describing the change of velocity, temperature, and concentration in systems with multiple independent variables. In chemical engineering, PDEs are commonly encountered, especially first and second-order equations, which are essential for understanding transport phenomena. Additionally, PDEs are used to model diffusive-advective transport equations in chemical systems, with applications in solving

steady-state conditions and addressing challenges like hyperbolic PDE systems and discontinuous solutions. Overall, PDEs are fundamental tools in chemistry for predicting and understanding complex dynamics at various spatial and temporal scales. PDEs in chemistry help explain system evolution at macroscopic scales, aiding in efficient computation-intensive tasks like prediction and control of physico-chemical processes.

Among PDEs, hyperbolic PDEs have a significant role in applicable sciences and engineering, and are applied in the formulation fundamental equations in atomic physics [1]. Telegraph equation is one of the high usage hyperbolic equation which is employed in the study of wave propagation of electric signals [2] and wave phenomena [3]. The telegraph partial differential equation has various applications in different fields. One application is in the mathematical modeling of transmission lines, where it is used to find the approximate solution of hyperbolic PDEs. Another application is in representing reaction-diffusion processes in engineering and biological disciplines. The telegraph equation is also used in signal analysis, wave propagation, and random walk problems. Additionally, it is applied in studying the influence of microwaves on signal transmission in telecommunication water. Furthermore, the telegraph equation is used in finance for non-linear transformations of classical telegraph processes, such as in option pricing. Since in most situations, it is difficult to solve telegraph equation explicitly, much efforts have been done to provide their accurate numerical solution. Different types of 1D telegraph equations have been solved via varied techniques including spectral Legendre-Galerkin algorithm [4], B-spline Galerkin [5], cubic B-spline finite elements [6], meshless local radial point interpolation [7], Chebyshev tau approximation [8], a combined technique based on meshless and finite difference method [9]. Solving 2D telegraph equation is more complicated than 1D telegraph equation and recently some articles have been published on the numerical solution of 2D telegraph equation. For instance, Yüzbaşı and Karaçayır used a Galerkin-like scheme to solve 2D version of telegraph equation in [10]. In [11], 2D telegraph equation with Dirichlet boundary conditions has been first turned into partial integro-differential equations (PIDEs) and then obtained PIDEs have been numerically solved via operational matrix method. The traditional meshfree scheme has been presented in [12], while the author of [13] combined meshless method with spectral collocation idea in order to provide the approximate solution of 2D time-fractional telegraph equation.

In many cases, there is uncertainty in real problems that must be included in mathematical models. All phenomena are modeled by deterministic functional equations, have some random factors that are ignored due to poor computational power. Therefore, it is interesting and necessary to consider stochastic effects and to study the impact of noise on regularities of the solutions and their longtime behaviors. In recent decades, by increasing demand to employ more suitable models and to gain more accurate results, a noise source was entered to integral equations (IEs), PDEs and ODEs and have been created stochastic IEs (SIEs), stochastic PDEs (SPDEs) and stochastic ODEs (SODEs).

This leads to considering the stochastic telegraph equations, which is defined by adding a noise term to the deterministic telegraph equations. On the other hand, derivatives of fractional order allow the memory and heredity qualities of various substances to be described. So, stochastic telegraph equations of fractional order are more suitable than integer-order stochastic telegraph equations. Solving stochastic functional equations exactly in many situations are impossible and it is necessary that some acceptable schemes are implemented to provide their approximate solution. Meshless methods based on radial basis functions (RBFs) have been developed to solve two-dimensional weakly singular SIEs [14]. In these methods, RBFs interpolation are used to estimate the unknown function and then obtained integrals are approximated via quadrature rules, therefore solving SIEs are reduced to solving a system of algebraic equations. Also, operational matrix method based on hat basis functions [15], hybrid functions [16], delta functions

[17], Bernoulli operationals [18], Euler polynomials [19] and other basis functions and polynomials have been applied to obtain the approximate solution of SIEs. The behavior of SPDEs has been simulated via meshless method based on RBFs [20], Galerkin approximation [21], and the dual reciprocity method [22]. Meshless method [23] and combination of finite difference and meshless method [24] have been developed to solve stochastic advection-diffusion equation, while wavelet Galerkin method has been used to estimate the solution of stochastic heat equation [25]. Unlike many applications of the telegraph equation, this equation has not been solved numerically so far. The authors have tried for the first time in this article to provide a suitable numerical method to approximate the solution of 2D stochastic space fractional telegraph equation.

Many approximate schemes have been employed to solve time-dependent PDEs numerically. In one of the numerical methods, space variables are discretized via different techniques such as finite difference, spectral, or meshless method but the time variable is leaved. This approach which converts time-dependent PDEs to a system of ODEs with appropriate initial conditions is called MOL. MOL is sometime considered as special finite difference method, but it is better than this method and has situated at semi-analytical method. MOL has been applied to obtain the numerical solution of some problems such as fractional diffusion equation [26, 27], parabolic equations [28] and Boussinesq equations [29].

2D stochastic space fractional telegraph equation is formulated as follows:

$$\frac{\partial^2 u(x,y,t)}{\partial t^2} + 2\mu\frac{\partial u(x,y,t)}{\partial t} + \theta^2 u(x,y,t) = \frac{\partial^\alpha u(x,y,t)}{\partial x^\alpha}$$
$$+ \frac{\partial^\beta u(x,y,t)}{\partial y^\beta} + k(x,y,t) + \sigma\frac{dB(t)}{dt}, \qquad (1)$$

where $(x,y,t) \in \Omega \times [0,T]$, $\Omega = [0,1] \times [0,1]$ is the space domain and $[0,T]$ is the time interval. μ, θ and σ are given constant numbers, $B(t)$ denotes Brownian motion process that is nowhere differentiable, $\frac{dB(t)}{dt}$ is called White Noise process that it dose note exist as a function of t. The function $k(x,y,t)$ is a known function while $u(x,y,t)$ is an unknown function which should be determined. $\frac{\partial^\alpha u(x,y,t)}{\partial x^\alpha}$ and $\frac{\partial^\beta u(x,y,t)}{\partial y^\beta}$ are the Caputo fractional derivatives of order α and β, $(1 < \alpha, \beta \le 2)$, that are respectively defined as follows [30, 31]:

$$\frac{\partial^\alpha u(x,y,t)}{\partial x^\alpha} = \frac{1}{\Gamma(2-\alpha)}\int_0^x (x-\eta)^{1-\alpha}\frac{\partial^2 u(\eta,y,t)}{\partial\eta^2}d\eta, \qquad (2)$$

and

$$\frac{\partial^\beta u(x,y,t)}{\partial y^\beta} = \frac{1}{\Gamma(2-\beta)}\int_0^y (y-\eta)^{1-\beta}\frac{\partial^2 u(x,\eta,t)}{\partial\eta^2}d\eta. \qquad (3)$$

The initial conditions are given by

$$\begin{cases} u(x,y,0) = f_1(x,y), & (x,y) \in \Omega, \\ u_t(x,y,0) = f_2(x,y), & (x,y) \in \Omega, \end{cases} \qquad (4)$$

and the Dirichlet boundary conditions are:

$$\begin{cases} u(0,y,t) = g_1(y,t), & u(1,y,t) = g_2(y,t), \\ u(x,0,t) = h_1(x,t), & u(x,1,t) = h_2(x,t), \end{cases} \qquad (5)$$

where f_i, g_i and h_i for $i = 1,2$ are known functions. Most important obstacle in solving Equation (1) is computational complexity due to stochastic term, fractional derivatives and

high dimension. In this article, a computational idea based on MOL and spline approximation is presented to derive the numerical solution of Equation (1) and then its error analysis is investigated.

The continuation of this work is as follows: A numerical method is expressed to solve 2D stochastic space fractional telegraph equation with appropriate initial and boundary conditions in Section 2. Error analysis of the mentioned scheme has been investigated in Section 3. Test problems and numerical results of the expressed method are carried out in Section 4. Finally, the conclusion of this study is collected in Section 5.

2 Numerical scheme

In this section, a numerical scheme is presented to approximate the solution of Equation (1) under the initial conditions (4) and the Dirichlet boundary conditions (5). In this approach, first consider two positive constant numbers M and N, then define the equidistance mesh points x_i and y_j as follows:

$$x_i = i\Delta x, \qquad i = 0, 1, \ldots, N,$$
$$y_j = j\Delta y, \qquad j = 0, 1, \ldots, M,$$

where $\Delta x = \frac{1}{N}$ and $\Delta y = \frac{1}{M}$ denote the spatial step sizes in x and y directions, respectively. By installing collocation points $x = x_i$ and $y = y_j$ into Equation (1), conclude

$$\frac{\partial^2 u(x_i, y_j, t)}{\partial t^2} + 2\mu \frac{\partial u(x_i, y_j, t)}{\partial t} + \theta^2 u(x_i, y_j, t) = \frac{\partial^\alpha u(x_i, y_j, t)}{\partial x^\alpha} + \frac{\partial^\beta u(x_i, y_j, t)}{\partial y^\beta}$$
$$+ k(x_i, y_j, t) + \sigma \frac{dB(t)}{dt}, \quad i = 1, 2, \ldots, N-1, \ \ j = 1, 2, \ldots, M-1. \quad (6)$$

Furthermore, the initial and boundary conditions are converted to

$$\begin{cases} u(x_i, y_j, 0) = f_1(x_i, y_j), \\ u_t(x_i, y_j, 0) = f_2(x_i, y_j), \\ u(x_0, y_j, t) = g_1(y_j, t), & u(x_N, y_j, t) = g_2(y_j, t), \\ u(x_i, y_0, t) = h_1(x_i, t), & u(x_i, y_M, t) = h_2(x_i, t). \end{cases} \quad (7)$$

Let $u_{i,j}(t) = u(x_i, y_j, t)$ and $k_{i,j}(t) = k(x_i, y_j, t)$ which $i = 0, 1, \ldots, N, j = 0, 1, \ldots, M$. By using these notations, Equation (6) can be written as follows:

$$u_{i,j}''(t) + 2\mu u_{i,j}'(t) + \theta^2 u_{i,j}(t) = \frac{\partial^\alpha u(x_i, y_j, t)}{\partial x^\alpha} + \frac{\partial^\beta u(x_i, y_j, t)}{\partial y^\beta} + k_{i,j}(t) + \sigma \frac{dB(t)}{dt}, \quad (8)$$

subject to the following initial conditions

$$\begin{cases} u_{i,j}(0) = f_1(x_i, y_j), & i = 1, 2, \ldots, N-1, \ \ j = 1, 2, \ldots, M-1, \\ u_{i,j}'(0) = f_2(x_i, y_j), & i = 1, 2, \ldots, N-1, \ \ j = 1, 2, \ldots, M-1. \end{cases} \quad (9)$$

Let $\mathscr{K}_{i,j} = \frac{\partial^\alpha u(x_i, y_j, t)}{\partial x^\alpha}$, $i = 1, 2, \ldots, N-1$, $j = 1, 2, \ldots, M-1$. Equation (2) yields

$$\mathscr{K}_{i,j} = \frac{\partial^\alpha u(x_i, y_j, t)}{\partial x^\alpha} = \frac{1}{\Gamma(2-\alpha)} \int_0^{x_i} (x_i - \eta)^{1-\alpha} \frac{\partial^2 u(\eta, y_j, t)}{\partial \eta^2} d\eta$$

$$= \frac{1}{\Gamma(2-\alpha)} \sum_{k=0}^{i-1} \int_{x_k}^{x_{k+1}} (x_i - \eta)^{1-\alpha} \frac{\partial^2 u(\eta, y_j, t)}{\partial \eta^2} d\eta. \quad (10)$$

The linear spline approximation of $\frac{\partial^2 u(\eta, y_j, t)}{\partial \eta^2}$ where $x_k \leq \eta \leq x_{k+1}$ is denoted by $\xi_{k,j}(\eta, t)$, and is as follows:

$$\frac{\partial^2 u(\eta, y_j, t)}{\partial \eta^2} \simeq \xi_{k,j}(\eta, t) = \frac{\eta - x_k}{\Delta x} \frac{\partial^2 u(x_{k+1}, y_j, t)}{\partial \eta^2} + \frac{x_{k+1} - \eta}{\Delta x} \frac{\partial^2 u(x_k, y_j, t)}{\partial \eta^2}.$$

Under continuity condition of $\frac{\partial^4 u(x,y,t)}{\partial x^4}$ yields [26]:

$$\frac{\partial^2 u(\eta, y_j, t)}{\partial \eta^2} = \xi_{k,j}(\eta, t) + O(\Delta x^2). \tag{11}$$

Inserting Equation (11) into Equation (10) yields:

$$\begin{aligned}
\mathscr{K}_{i,j} &= \frac{1}{\Gamma(2-\alpha)} \sum_{k=0}^{i-1} \int_{x_k}^{x_{k+1}} (x_i - \eta)^{1-\alpha} \Big[\xi_{k,j}(\eta, t) + O(\Delta x^2) \Big] d\eta \\
&= \frac{\Delta x^{2-\alpha}}{\Gamma(4-\alpha)} \sum_{k=0}^{i} a_{i,k} \frac{\partial^2 u(x_k, y_j, t)}{\partial \eta^2} + \frac{x_i^{2-\alpha}}{\Gamma(3-\alpha)} O(\Delta x^2),
\end{aligned} \tag{12}$$

where the constant coefficients $a_{i,k}$ where $k = 0, 1, \ldots, i$ are computed as follows:

$$a_{i,k} = \begin{cases} (i-1)^{3-\alpha} - i^{2-\alpha}(i-3+\alpha), & k = 0, \\ (i-k+1)^{3-\alpha} - 2(i-k)^{3-\alpha} + (i-k-1)^{3-\alpha}, & 1 \leq k \leq i-1, \\ 1, & k = i. \end{cases}$$

Theorem 2.1. The definition of the constant coefficients $a_{i,k}$ imply that:

$$\sum_{k=0}^{i} a_{i,k} = (3-\alpha) i^{2-\alpha}. \tag{13}$$

Proof. It follows from the definition of coefficients $a_{i,k}$ that

$$\begin{aligned}
\sum_{k=0}^{i} a_{i,k} &= (i-1)^{3-\alpha} - i^{2-\alpha}(i-3+\alpha) + \sum_{k=1}^{i-1} (i-k+1)^{3-\alpha} \\
&\quad - 2(i-k)^{3-\alpha} + (i-k-1)^{3-\alpha} + 1 = (i-1)^{3-\alpha} - i^{2-\alpha}(i-3+\alpha) \\
&\quad + \sum_{k=1}^{i-1} (i-k+1)^{3-\alpha} - (i-k)^{3-\alpha} - \sum_{k=1}^{i-1} (i-k)^{3-\alpha} - (i-k-1)^{3-\alpha} + 1.
\end{aligned}$$

From telescoping sum rule can be concluded that

$$\begin{aligned}
\sum_{k=0}^{i} a_{i,k} &= (i-1)^{3-\alpha} - i^{2-\alpha}(i-3+\alpha) + i^{3-\alpha} - 1 - (i-1)^{3-\alpha} + 1 \\
&= (3-\alpha) i^{2-\alpha}.
\end{aligned}$$

∎

Now, we should find an appropriate approximation for second-order derivative $\frac{\partial^2 u(x_k, y_j, t)}{\partial \eta^2}$ in Equation (12). For $k = 0$, use forward finite difference formula to estimate second-order derivative, i.e.,

$$\frac{\partial^2 u(x_0, y_j, t)}{\partial \eta^2} = \frac{-u(x_3, y_j, t) + 4u(x_2, y_j, t) - 5u(x_1, y_j, t) + 2u(x_0, y_j, t)}{\Delta x^2} + O(\Delta x^2)$$

$$= \frac{-u_{3,j}(t) + 4u_{2,j}(t) - 5u_{1,j}(t) + 2u_{0,j}(t)}{\Delta x^2} + O(\Delta x^2)$$

$$= \delta_{0,j}(t) + O(\Delta x^2).$$

For $k = 1, 2, \ldots, N-1$, use central finite difference formula, i.e.,

$$\frac{\partial^2 u(x_k, y_j, t)}{\partial \eta^2} = \frac{u(x_{k+1}, y_j, t) - 2u(x_k, y_j, t) + u(x_{k-1}, y_j, t)}{\Delta x^2} + O(\Delta x^2)$$

$$= \frac{u_{k+1,j}(t) - 2u_{k,j}(t) + u_{k-1,j}(t)}{\Delta x^2} + O(\Delta x^2) = \delta_{k,j}(t) + O(\Delta x^2). \tag{14}$$

Inserting Equation (14) into Equation (12) yields:

$$\mathscr{K}_{i,j} = \frac{\Delta x^{2-\alpha}}{\Gamma(4-\alpha)} \sum_{k=0}^{i} a_{i,k} \left[\delta_{k,j}(t) + O(\Delta x^2) \right] + \frac{x_i^{2-\alpha}}{\Gamma(3-\alpha)} O(\Delta x^2)$$

$$= \frac{\Delta x^{2-\alpha}}{\Gamma(4-\alpha)} \sum_{k=0}^{i} a_{i,k} \delta_{k,j}(t) + \frac{\Delta x^{2-\alpha} O(\Delta x^2)}{\Gamma(4-\alpha)} \sum_{k=0}^{i} a_{i,k} + \frac{x_i^{2-\alpha}}{\Gamma(3-\alpha)} O(\Delta x^2). \tag{15}$$

It follows from Theorem 2.1 and Equation (15) that:

$$\mathscr{K}_{i,j} = \frac{\Delta x^{2-\alpha}}{\Gamma(4-\alpha)} \sum_{k=0}^{i} a_{i,k} \delta_{k,j}(t) + \frac{2x_i^{2-\alpha}}{\Gamma(3-\alpha)} O(\Delta x^2). \tag{16}$$

In the next step, we should provide an appropriate approximation for $\frac{\partial^\beta u(x_i, y_j, t)}{\partial y^\beta}$ in Equation (8). Let $\mathscr{H}_{i,j} = \frac{\partial^\beta u(x_i, y_j, t)}{\partial y^\beta}$, $i = 1, 2, \ldots, N-1$, $j = 1, 2, \ldots, M-1$. Using Equation (3) yields:

$$\mathscr{H}_{i,j} = \frac{\partial^\beta u(x_i, y_j, t)}{\partial y^\beta} = \frac{1}{\Gamma(2-\beta)} \int_0^{y_j} (y_j - \eta)^{1-\beta} \frac{\partial^2 u(x_i, \eta, t)}{\partial \eta^2} d\eta$$

$$= \frac{1}{\Gamma(2-\beta)} \sum_{k=0}^{j-1} \int_{y_k}^{y_{k+1}} (y_j - \eta)^{1-\beta} \frac{\partial^2 u(x_i, \eta, t)}{\partial \eta^2} d\eta. \tag{17}$$

Let $\zeta_{i,k}(\eta, t)$ as the linear spline approximation of $\frac{\partial^2 u(x_i, \eta, t)}{\partial \eta^2}$ where $y_k \leq \eta \leq y_{k+1}$. Thus

$$\frac{\partial^2 u(x_i, \eta, t)}{\partial \eta^2} \simeq \zeta_{i,k}(\eta, t) = \frac{\eta - y_k}{\Delta y} \frac{\partial^2 u(x_i, y_{k+1}, t)}{\partial \eta^2} + \frac{y_{k+1} - \eta}{\Delta y} \frac{\partial^2 u(x_i, y_k, t)}{\partial \eta^2}.$$

Similarly, under continuity condition of $\frac{\partial^4 u(x, y, t)}{\partial y^4}$, we obtain [26]:

$$\frac{\partial^2 u(x_i, \eta, t)}{\partial \eta^2} = \zeta_{i,k}(\eta, t) + O(\Delta y^2). \tag{18}$$

Substituting Equation (18) into Equation (17) yields:

$$\mathcal{H}_{i,j} = \frac{1}{\Gamma(2-\beta)} \sum_{k=0}^{j-1} \int_{y_k}^{y_{k+1}} (y_j - \eta)^{1-\beta} \Big[\zeta_{i,k}(\eta, t) + O(\Delta y^2) \Big] d\eta$$

$$= \frac{\Delta y^{2-\beta}}{\Gamma(4-\beta)} \sum_{k=0}^{j} b_{j,k} \frac{\partial^2 u(x_i, y_k, t)}{\partial \eta^2} + \frac{y_j^{2-\beta}}{\Gamma(3-\beta)} O(\Delta y^2), \qquad (19)$$

where the constant coefficients $b_{j,k}$ where $k = 0, 1, \ldots, j$ are calculated as follows:

$$b_{j,k} = \begin{cases} (j-1)^{3-\beta} - j^{2-\beta}(j-3+\beta), & k = 0, \\ (j-k+1)^{3-\beta} - 2(j-k)^{3-\beta} + (j-k-1)^{3-\beta}, & 1 \le k \le j-1, \\ 1, & k = j. \end{cases}$$

Theorem 2.2. The definition of the constant coefficients $b_{j,k}$ imply that:

$$\sum_{k=0}^{j} b_{j,k} = (3-\beta) j^{2-\beta}. \qquad (20)$$

Proof. The proof of this theorem is done similar to the proof of Theorem 2.1.   ∎

In this stage, estimate the second order derivative $\frac{\partial^2 u(x_i, y_k, t)}{\partial \eta^2}$ for $k = 0, 1, \ldots, M-1$. Similarly, use forward formula for $k = 0$ and yields

$$\frac{\partial^2 u(x_i, y_0, t)}{\partial \eta^2} = \frac{-u(x_i, y_3, t) + 4u(x_i, y_2, t) - 5u(x_i, y_1, t) + 2u(x_i, y_0, t)}{\Delta y^2} + O(\Delta y^2)$$

$$= \frac{-u_{i,3}(t) + 4u_{i,2}(t) - 5u_{i,1}(t) + 2u_{i,0}(t)}{\Delta y^2} + O(\Delta y^2)$$

$$= \gamma_{i,0}(t) + O(\Delta y^2).$$

Furthermore, central formula is used for $k = 1, 2, \ldots, M-1$, i.e.,

$$\frac{\partial^2 u(x_i, y_k, t)}{\partial \eta^2} = \frac{u(x_i, y_{k+1}, t) - 2u(x_i, y_k, t) + u(x_i, y_{k-1}, t)}{\Delta y^2} + O(\Delta y^2)$$

$$= \frac{u_{i,k+1}(t) - 2u_{i,k}(t) + u_{i,k-1}(t)}{\Delta y^2} + O(\Delta y^2) = \gamma_{i,k}(t) + O(\Delta y^2). \qquad (21)$$

Substituting Equation (21) into Equation (19) and using Theorem 2.2 yields:

$$\mathcal{H}_{i,j} = \frac{\Delta y^{2-\beta}}{\Gamma(4-\beta)} \sum_{k=0}^{j} b_{j,k} \Big[\gamma_{i,k}(t) + O(\Delta y^2) \Big] + \frac{y_j^{2-\beta}}{\Gamma(3-\beta)} O(\Delta y^2)$$

$$= \frac{\Delta y^{2-\beta}}{\Gamma(4-\beta)} \sum_{k=0}^{j} b_{j,k} \gamma_{i,k}(t) + \frac{\Delta y^{2-\beta} O(\Delta y^2)}{\Gamma(4-\beta)} \sum_{k=0}^{j} b_{j,k} + \frac{y_j^{2-\beta}}{\Gamma(3-\beta)} O(\Delta y^2)$$

$$= \frac{\Delta y^{2-\beta}}{\Gamma(4-\beta)} \sum_{k=0}^{j} b_{j,k} \gamma_{i,k}(t) + \frac{2 y_j^{2-\beta}}{\Gamma(3-\beta)} O(\Delta y^2). \qquad (22)$$

Now, insert approximations of $\mathscr{K}_{i,j}$ and $\mathscr{H}_{i,j}$, which provided in Equation (16) and Equation (22) respectively, into Equation(8), and get the following system of $\mathcal{L} = (N-1) \times (M-1)$ IVPs

$$u_{i,j}''(t) + 2\mu u_{i,j}'(t) + \theta^2 u_{i,j}(t) = \frac{\Delta x^{2-\alpha}}{\Gamma(4-\alpha)} \sum_{k=0}^{i} a_{i,k} \delta_{k,j}(t) + \frac{2x_i^{2-\alpha}}{\Gamma(3-\alpha)} O(\Delta x^2)$$

$$+ \frac{\Delta y^{2-\beta}}{\Gamma(4-\beta)} \sum_{k=0}^{j} b_{j,k} \gamma_{i,k}(t) + \frac{2y_j^{2-\beta}}{\Gamma(3-\beta)} O(\Delta y^2) + k_{i,j}(t) + \sigma \frac{dB(t)}{dt}, \qquad (23)$$

subject to the initial conditions which are given in Equation (9).

For $i = 1, 2, \ldots, N-1$ and $j = 1, 2, \ldots, M-1$, define $\rho_i(t)$, $\varrho_j(t)$ and $\omega_{i,j}(t)$ as follows:

$$\rho_i(t) = \frac{\Delta y^{2-\beta}}{\Gamma(4-\beta)} b_{M-1,M-1} h_2(x_i, t), \qquad \varrho_j(t) = \frac{\Delta x^{2-\alpha}}{\Gamma(4-\alpha)} a_{N-1,N-1} g_2(y_j, t),$$

and

$$\omega_{i,j}(t) = (2a_{i,0} + a_{i,1}) \frac{\Delta x^{-\alpha}}{\Gamma(4-\alpha)} g_1(y_j, t) + (2b_{j,0} + b_{j,1}) \frac{\Delta y^{-\beta}}{\Gamma(4-\beta)} h_1(x_i, t),$$

and put

$$\overrightarrow{W}(t) = [\omega_{1,1}(t), \omega_{1,2}(t), \ldots, \omega_{1,M-1}(t) + \rho_1, \omega_{2,1}(t), \omega_{2,2}(t), \ldots, \omega_{2,M-1}(t) + \rho_2$$

$$, \ldots, \omega_{N-1,1}(t) + \varrho_1, \omega_{N-1,2}(t) + \varrho_2, \ldots, \omega_{N-1,M-1}(t) + \rho_{N-1} + \varrho_{M-1}]^T.$$

For $i = 1, 2, \ldots, N-1$ and $j = 1, 2, \ldots, M-1$, let

$$\upsilon_{i,j} = \frac{2x_i^{2-\alpha}}{\Gamma(3-\alpha)} O(\Delta x^2) + \frac{2y_j^{2-\beta}}{\Gamma(3-\beta)} O(\Delta y^2),$$

and define vector $\overrightarrow{V}$ as follows

$$\overrightarrow{V} = [\upsilon_{1,1}, \upsilon_{1,2}, \ldots, \upsilon_{1,M-1}, \ldots, \upsilon_{N-1,1}, \upsilon_{N-1,2}, \ldots, \upsilon_{N-1,M-1}]^T.$$

Furthermore, define the following vectors and matrix

$$\overrightarrow{U}(t) = \begin{pmatrix} u_{1,1}(t) \\ u_{1,2}(t) \\ \vdots \\ u_{N-1,M-1}(t) \end{pmatrix}_{\mathcal{L} \times 1}, \qquad \overrightarrow{K}(t) = \begin{pmatrix} k_{1,1}(t) + \sigma \frac{dB(t)}{dt} \\ k_{1,2}(t) + \sigma \frac{dB(t)}{dt} \\ \vdots \\ k_{N-1,M-1}(t) + \sigma \frac{dB(t)}{dt} \end{pmatrix}_{\mathcal{L} \times 1},$$

$$\mathcal{M} = \begin{pmatrix} 2\mu & & & \\ & 2\mu & & \\ & & \ddots & \\ & & & 2\mu \end{pmatrix}_{\mathcal{L} \times \mathcal{L}}.$$

By using the above definitions, the system of $\mathcal{L}$ IVPs (23) with initial conditions (9) can be written in the following matrix form:

$$\begin{cases} \overrightarrow{U''}(t) + \mathcal{M}\overrightarrow{U'}(t) + \mathcal{N}\overrightarrow{U}(t) = \overrightarrow{V} + \overrightarrow{K}(t) + \overrightarrow{W}(t), \\ \overrightarrow{U}(0) = \overrightarrow{F_1}, \\ \overrightarrow{U'}(0) = \overrightarrow{F_2}, \end{cases} \qquad (24)$$

where $\overrightarrow{F_1}$ and $\overrightarrow{F_2}$ are two vectors of order $\mathcal{L} \times 1$ as follows:

$$\overrightarrow{F_1} = [f_1(x_1, y_1), f_1(x_1, y_2), \ldots, f_1(x_1, y_{M-1}), \ldots, f_1(x_{N-1}, y_1), \ldots, f_1(x_{N-1}, y_{M-1})]^T,$$
$$\overrightarrow{F_2} = [f_2(x_1, y_1), f_2(x_1, y_2), \ldots, f_2(x_1, y_{M-1}), \ldots, f_2(x_{N-1}, y_1), \ldots, f_2(x_{N-1}, y_{M-1})]^T.$$

The matrix $\mathcal{N}$ in Equation (24) is a block matrix of order $\mathcal{L} \times \mathcal{L}$ defined as:

$$\mathcal{N} = \begin{pmatrix} A_{1,1} + C & A_{1,2} & A_{1,3} & O & \ldots & O \\ A_{2,1} & A_{2,2} + C & A_{2,3} & O & \ldots & O \\ \vdots & \vdots & \vdots & \vdots & \ddots & \vdots \\ A_{N-1,1} & A_{N-1,2} & A_{N-1,3} & A_{N-1,4} & \ldots & A_{N-1,N-1} + C \end{pmatrix}, \tag{25}$$

where O is zero matrix of order $(M-1) \times (M-1)$, the matrix C is defined as:

$$C = \frac{\Delta y^{-\beta}}{\Gamma(4-\beta)} BX + \frac{\Delta y^{-\beta}}{\Gamma(4-\beta)} D + \Theta,$$

where X, B, D and Θ are matrices of order $(M-1) \times (M-1)$ and are defined as:

$$X = \begin{pmatrix} 2 & -1 & & & \\ -1 & 2 & -1 & & \\ & \ddots & \ddots & \ddots & \\ & & -1 & 2 & -1 \\ & & & -1 & 2 \end{pmatrix}, \quad D = \begin{pmatrix} 5b_{1,0} & -4b_{1,0} & b_{1,0} & 0 & \ldots & 0 \\ 5b_{2,0} & -4b_{2,0} & b_{2,0} & 0 & \ldots & 0 \\ \vdots & \vdots & \vdots & \vdots & \ddots & \vdots \\ 5b_{M-1,0} & -4b_{M-1,0} & b_{M-1,0} & 0 & \ldots & 0 \end{pmatrix},$$

$$\Theta = \begin{pmatrix} \theta^2 & & & \\ & \theta^2 & & \\ & & \ddots & \\ & & & \theta^2 \end{pmatrix},$$

and B is a lower triangular matrix which is defined as:

$$B = [b_{ij}], \quad b_{ij} = \begin{cases} 0, & i < j, \\ b_{i,j}, & i \geq j. \end{cases}$$

Furthermore $A_{i,j}$ in Equation (25) is diagonal matrix of order $(M-1) \times (M-1)$ which its diagonal elements are ij th element of matrix E, and matrix E is defined as:

$$E = \frac{\Delta x^{-\alpha}}{\Gamma(4-\alpha)} AX + \frac{\Delta x^{-\alpha}}{\Gamma(4-\alpha)} F,$$

where A and F are matrices of order $(M-1) \times (M-1)$ and are defined as:

$$F = \begin{pmatrix} 5a_{1,0} & -4a_{1,0} & a_{1,0} & 0 & \ldots & 0 \\ 5a_{2,0} & -4a_{2,0} & a_{2,0} & 0 & \ldots & 0 \\ \vdots & \vdots & \vdots & \vdots & \ddots & \vdots \\ 5a_{M-1,0} & -4a_{M-1,0} & a_{M-1,0} & 0 & \ldots & 0 \end{pmatrix}, \quad A = [a_{ij}], \quad a_{ij} = \begin{cases} 0, & i < j, \\ a_{i,j}, & i \geq j. \end{cases}$$

To determine the exact values of $u_{0,j}(t)$, $u_{N,j}(t)$, $u_{i,0}(t)$ and $u_{i,M}(t)$ for $i = 0, 1, \ldots, N$ and $j = 0, 1, \ldots, M$, employ boundary conditions given in Equation (7). Furthermore, the approximate

values of $u_{i,j}(t)$ for $i = 1, 2, \ldots, N - 1$ and $j = 1, 2, \ldots, M - 1$ can be obtained by solving the system of IVPs (24), numerically. Since the vector $\overrightarrow{V}$ in system (24) contains the unknown error term $O(\Delta x^2 + \Delta y^2)$, we ignore this vector and solve the following system of IVPs to approximate the values of $u_{i,j}(t)$,

$$
\begin{cases}
\overrightarrow{\tilde{U}''}(t) + \mathcal{M}\overrightarrow{\tilde{U}'}(t) + \mathcal{N}\overrightarrow{\tilde{U}}(t) = \overrightarrow{K}(t) + \overrightarrow{W}(t), \\
\overrightarrow{\tilde{U}}(0) = \overrightarrow{F_1}, \\
\overrightarrow{\tilde{U}'}(0) = \overrightarrow{F_2}.
\end{cases}
\tag{26}
$$

3   Error analysis

In this section, we investigate that how ignoring the unknown error therm $\overrightarrow{V}$ can affect the numerical solution of Equation (1). Define $\overrightarrow{e}(t) = \overrightarrow{U}(t) - \overrightarrow{\tilde{U}}(t)$. By subtracting Equation (24) from Equation (26), one see that the error function $\overrightarrow{e}(t)$ satisfies in the following linear system of IVPs with zero initial conditions

$$
\begin{cases}
\overrightarrow{e''}(t) + \mathcal{M}\overrightarrow{e'}(t) + \mathcal{N}\overrightarrow{e}(t) = \overrightarrow{V}, \\
\overrightarrow{e}(0) = 0, \\
\overrightarrow{e'}(0) = 0.
\end{cases}
\tag{27}
$$

Let $\overrightarrow{e}(t) = \psi_1(t)$ and $\overrightarrow{e'}(t) = \psi_2(t)$, then the homogenous second order IVPs system (27) can be written as the following linear system of IVPs of first order

$$
\frac{d}{dt}\begin{pmatrix} \psi_1(t) \\ \psi_2(t) \end{pmatrix} = \underbrace{\begin{pmatrix} O & I \\ -\mathcal{N} & -\mathcal{M} \end{pmatrix}}_{\Upsilon}\begin{pmatrix} \psi_1(t) \\ \psi_2(t) \end{pmatrix}.
\tag{28}
$$

Define $\Psi(t) = \begin{pmatrix} \psi_1(t) \\ \psi_2(t) \end{pmatrix}$. So, the following linear system of IVPs of the first order can be obtained:

$$
\begin{cases}
\Psi'(t) = \Upsilon\Psi(t), \\
\Psi(0) = 0.
\end{cases}
\tag{29}
$$

Suppose that $\lambda_1, \lambda_2, \ldots, \lambda_{2\mathcal{L}}$ be the distinct eigenvalues of matrix Υ with the corresponding eigenvectors $\overrightarrow{v}_1, \overrightarrow{v}_2, \ldots, \overrightarrow{v}_{2\mathcal{L}}$. Hence, the exact solution of linear system of IVPs (29) can be written as:

$$
\overrightarrow{\Psi}(t) = \sum_{i=1}^{2\mathcal{L}} c_i \exp(\lambda_i t)\overrightarrow{v}_i,
\tag{30}
$$

where the unknown coefficients c_i for $i = 1, 2, \ldots, 2\mathcal{L}$ are determined via using initial value conditions. The first $\mathcal{L}$ rows of $\overrightarrow{\Psi}(t)$ denote the obtained solution for $\overrightarrow{e}(t) = \psi_1(t)$. Suppose that vectors $\overrightarrow{z}_1, \overrightarrow{z}_2, \ldots, \overrightarrow{z}_{2\mathcal{L}}$ are truncated vectors of vectors $\overrightarrow{v}_1, \overrightarrow{v}_2, \ldots, \overrightarrow{v}_{2\mathcal{L}}$ of order $\mathcal{L} \times 1$. Thus, the exact solution of second-order linear system of IVPs (27) can be expanded as follows:

$$
\overrightarrow{e}(t) = \sum_{i=1}^{2\mathcal{L}} c_i \exp(\lambda_i t)\overrightarrow{z}_i + \overrightarrow{d}_1 + \overrightarrow{d}_2 t,
\tag{31}
$$

Table 1: Values of $\|\mathcal{N}^{-1}\|_\infty$ for different values of M, N and α, β with $\theta = 1$.

$M = N$	$\alpha = \beta = 1.3$	$\alpha = \beta = 1.4$	$\alpha = \beta = 1.5$	$\alpha = \beta = 1.6$	$\alpha = \beta = 1.8$	$\alpha = \beta = 2$
40	0.1405	0.0236	0.0103	0.0061	0.0022	0.0012
50	0.1146	0.0174	0.0074	0.0043	0.0015	0.0007
60	0.0952	0.0135	0.0056	0.0032	0.0011	0.0005
70	0.0804	0.0109	0.0045	0.0025	0.0008	0.0004
80	0.0690	0.0090	0.0037	0.0020	0.0006	0.0003
90	0.0599	0.0077	0.0031	0.0017	0.0005	0.0002
100	0.0527	0.0060	0.0026	0.0014	0.0004	0.0001

where the initial conditions are used to determine the unknown coefficients $c_i, i = 1, 2, \ldots, 2\mathcal{L}$, and the vectors $\overrightarrow{a}_1$ and $\overrightarrow{a}_2$ are unknown constant vectors such that:

$$\mathcal{N} \overrightarrow{a}_2 = 0, \qquad \mathcal{N} \overrightarrow{a}_1 = \overrightarrow{V} - \mathcal{M} \overrightarrow{a}_2.$$

Non-singularity properties of matrix $\mathcal{N}$ yields:

$$\overrightarrow{a}_2 = 0, \qquad \overrightarrow{a}_1 = \mathcal{N}^{-1} \overrightarrow{V}. \tag{32}$$

Inserting Equation (32) into Equation (31) conclude:

$$\overrightarrow{e}(t) = \sum_{i=1}^{2\mathcal{L}} c_i \exp(\lambda_i t) \overrightarrow{z}_i + \mathcal{N}^{-1} \overrightarrow{V}, \tag{33}$$

where $\overrightarrow{V} \simeq O(\Delta x^2 + \Delta y^2)$. So

$$\overrightarrow{e}(t) = \sum_{i=1}^{2\mathcal{L}} c_i \exp(\lambda_i t) \overrightarrow{z}_i + \mathcal{N}^{-1} O(\Delta x^2 + \Delta y^2). \tag{34}$$

From Equation (34), we have:

$$\|\overrightarrow{e}(t)\|_\infty \le \epsilon + \|\mathcal{N}^{-1}\|_\infty O(\Delta x^2 + \Delta y^2), \qquad t > 0,$$

such that as t increases, ϵ tends to zero with exponential order. On the other hand, we numerically demonstrate in Table 1 that the infinity norm of $\mathcal{N}^{-1}$, which dependent only on α and β, is bounded. Thus

$$\|\overrightarrow{e}(t)\|_\infty \le \epsilon + \kappa O(\Delta x^2 + \Delta y^2),$$

where κ denotes the upper error bound of $\|\mathcal{N}^{-1}\|_\infty$. Hence, for sufficiently small values of Δx and Δy, we have:

$$\|\overrightarrow{U}(t) - \overrightarrow{\overline{U}}(t)\|_\infty \simeq O(\Delta x^2 + \Delta y^2).$$

4 Test problems

In this section, two test problems are given to test the maximum error and computational convergence order of the proposed technique on these problems. The effect of increasing M and N on accuracy of the described method are checked by performing the mentioned method for

different values of M and N. Our criterion to measure accuracy of this scheme is maximum error which is defined as follows:

$$L_\infty(x,y,t) = \|u(x,y,t) - \tilde{u}(x,y,t)\|_\infty = \max_{\substack{0 \le i \le N \\ 0 \le j \le M}} |u(x_i,y_j,t) - \tilde{u}(x_i,y_j,t)|,$$

where t is fixed time, $u(x,y,t)$ and $\tilde{u}(x,y,t)$ denote the exact solution and approximate solution of 2D stochastic space fractional telegraph equation, respectively. Also, the computational order of the presented method have been calculated as follows:

$$C_x - \text{order} = \log_2\Big(\frac{L_\infty(2\Delta x, \Delta y, t)}{L_\infty(\Delta x, \Delta y, t)}\Big), \qquad C_y - \text{order} = \log_2\Big(\frac{L_\infty(\Delta x, 2\Delta y, t)}{L_\infty(\Delta x, \Delta y, t)}\Big).$$

All the numerical calculations are performed on an Intel CORE i7 laptop by running a code written in MATLAB 7.11.0.584 (R2010b) software.

Example 4.1. Consider the telegraph Equation (1) defined on the domain $\Omega \times [0,1]$, and

$$k(x,y,t) = 2\mu + \theta^2(x^2 + y^2 + t) - \frac{2x^{2-\alpha}}{\Gamma(3-\alpha)} - \frac{2y^{2-\beta}}{\Gamma(3-\beta)} - \sigma\frac{dB(t)}{dt}.$$

The initial and boundary conditions are given by

$$\begin{cases} u(x,y,0) = x^2 + y^2, \\ u_t(x,y,0) = 1, \end{cases}$$

and

$$\begin{cases} u(0,y,t) = y^2 + t, & u(1,y,t) = 1 + y^2 + t, \\ u(x,0,t) = x^2 + t, & u(x,1,t) = x^2 + 1 + t. \end{cases}$$

The exact solution of this problem is $u(x,y,t) = x^2 + y^2 + t$. This example has been solved for $\mu = \theta = \sigma = 1$ and different values of α, β, M and N and obtained results have been reported in tables and figures. To investigate the effect of increasing the value of N on the approximate solution, consider a constant value for $M = 20$ and run the Matlab codes for different values of N and different values of fractional derivatives α and β, and report the obtained results in Table 2. Also, the error figures for $M = 20, N = 160$ and different values of α and β have been plotted in Figure 1. The effect of increasing M in approximate solution have been investigated in Table 3. From the reported results in Tables 2 and 3 can be conclude that by increasing the values of M and N, and consequently decreasing the values of spatial step sizes in x and y directions, the values of maximum error are reduced and more accurate results are provided. Also, it conclude that the computational convergence order is about 2. The behaviour of absolute error of described method for $u(0.5, 0.5, t)$ are depicted in Figure 2, where $0 \le t \le 1$ and $M = N = 10$ and $\alpha = \beta = 1.1, 1.2$ (left) and $\alpha = \beta = 1.9, 2$ (Right).

Example 4.2. Consider the telegraph Equation (1) defined on the domain $\Omega \times [0,1]$, and

$$k(x,y,t) = -\pi^2 x^2 y^3 \sin(\pi t) + 2\mu\pi x^2 y^3 \cos(\pi t) + \theta^2 x^2 y^3 \sin(\pi t)$$
$$- \frac{2x^{2-\alpha}y^3 \sin(\pi t)}{\Gamma(3-\alpha)} - \frac{6x^2 y^{3-\beta}\sin(\pi t)}{\Gamma(4-\beta)} - \sigma\frac{dB(t)}{dt}.$$

The initial and boundary conditions are given by

$$\begin{cases} u(x,y,0) = 0, \\ u_t(x,y,0) = \pi x^2 y^3, \end{cases}$$

Table 2: Numerical results of Example 4.1 with $M = 20$ at final time $T = 1$.

	$\alpha = \beta = 1.1$		$\alpha = \beta = 1.2$		$\alpha = \beta = 1.9$		$\alpha = \beta = 2$	
N	L_∞-error	C_x-order	L_∞-error	C_x-order	L_∞-error	C_x-order	L_∞-error	C_x-order
10	2.3547×10^{-3}	——	1.0842×10^{-3}	——	8.5234×10^{-4}	——	4.5281×10^{-4}	——
20	6.0172×10^{-4}	1.9684	2.5901×10^{-4}	2.0655	2.1236×10^{-4}	2.0049	1.1486×10^{-4}	1.9790
40	1.4532×10^{-4}	2.0499	6.5542×10^{-5}	1.9825	5.4428×10^{-5}	1.9640	3.0541×10^{-5}	1.9110
80	3.4205×10^{-5}	2.0870	1.5367×10^{-5}	2.0925	1.2074×10^{-5}	2.1724	7.1227×10^{-6}	2.1002
160	7.9530×10^{-6}	2.1046	4.0504×10^{-6}	1.9236	2.8110×10^{-6}	2.1027	1.7582×10^{-6}	2.0183

Table 3: Numerical results of Example 4.1 with $N = 10$ at final time $T = 1$.

|	$\alpha = \beta = 1.1$		$\alpha = \beta = 1.2$		$\alpha = \beta = 1.9$		$\alpha = \beta = 2$	
M	L_∞-error	C_y-order	L_∞-error	C_y-order	L_∞-error	C_y-order	L_∞-error	C_y-order
10	3.2571×10^{-2}	——	2.5427×10^{-2}	——	9.4735×10^{-3}	——	6.2541×10^{-3}	——
20	8.5461×10^{-3}	1.9302	5.9704×10^{-3}	2.0905	2.1928×10^{-3}	2.1111	1.4129×10^{-3}	2.1461
40	2.0281×10^{-3}	2.0751	1.5453×10^{-3}	1.9499	6.0598×10^{-4}	1.8554	3.7149×10^{-4}	1.9273
80	5.0703×10^{-4}	2.0000	3.4147×10^{-4}	2.1781	1.5735×10^{-4}	1.9453	9.5412×10^{-5}	1.9611
160	1.2849×10^{-4}	1.9804	9.0893×10^{-5}	1.9095	4.1031×10^{-5}	1.9392	2.1204×10^{-5}	2.1698
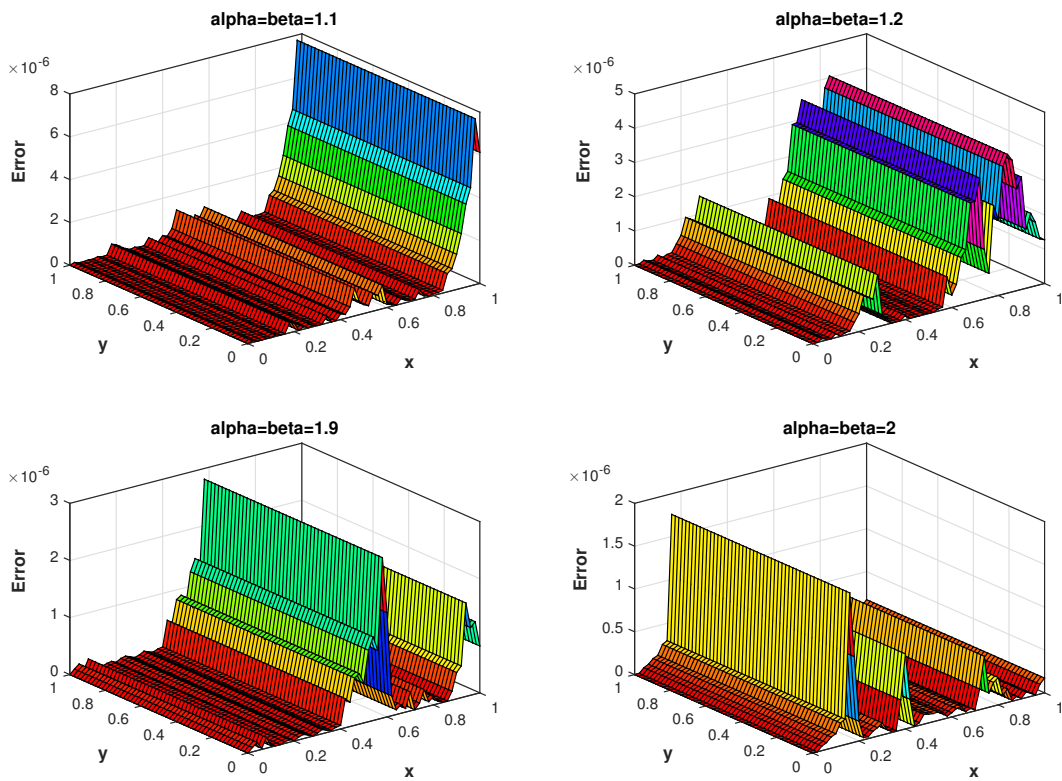
Figure 1: Absolute error of Example 4.1 for $M = 20, N = 160$ and different values of α and β at final time $T = 1$.
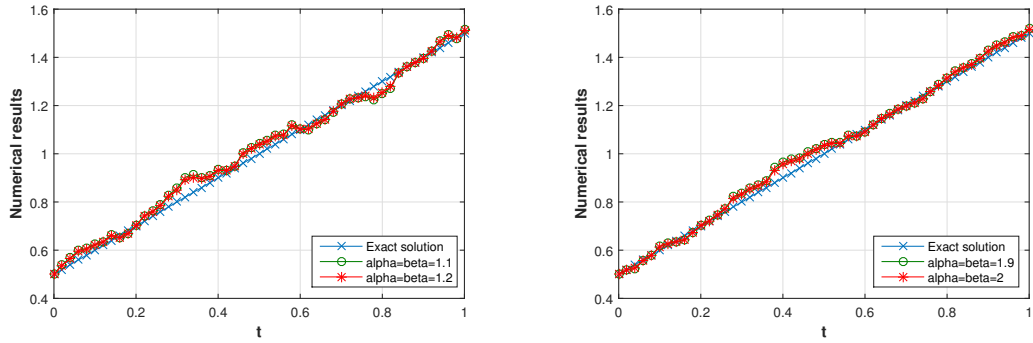
Figure 2: Absolute error at $x = y = 0.5$ of Example 4.1 for different values of α and β with $M = N = 10$.

Table 4: Numerical results of Example 4.2 with $M = 20$ at final time $T = 1$.

N	$\alpha = \beta = 1.1$		$\alpha = \beta = 1.2$		$\alpha = \beta = 1.9$		$\alpha = \beta = 2$	
	L_∞-error	C_x-order	L_∞-error	C_x-order	L_∞-error	C_x-order	L_∞-error	C_x-order
10	4.9542×10^{-3}	———	1.8935×10^{-3}	———	1.2039×10^{-3}	———	2.9546×10^{-4}	———
20	1.1284×10^{-3}	2.1343	3.9497×10^{-4}	2.2612	3.2548×10^{-4}	1.8870	7.6642×10^{-5}	1.9467
40	2.8243×10^{-4}	1.9983	8.9543×10^{-5}	2.1410	7.4512×10^{-5}	2.1270	2.1245×10^{-5}	1.8510
80	6.2204×10^{-5}	2.1828	2.5548×10^{-5}	1.8093	1.5842×10^{-5}	2.2337	5.9912×10^{-6}	1.8262
160	1.3263×10^{-5}	2.2296	5.4918×10^{-6}	2.2178	3.9018×10^{-6}	2.0215	1.5311×10^{-6}	1.9682

and

$$\begin{cases} u(0, y, t) = 0, & u(1, y, t) = y^3 \sin(\pi t), \\ u(x, 0, t) = 0, & u(x, 1, t) = x^2 \sin(\pi t). \end{cases}$$

The exact solution of this problem is $u(x, y, t) = x^2 y^3 \sin(\pi t)$. This example has been solved for $\mu = \theta = \sigma = 1$ and different values of α, β, M and N and obtained results have been reported in tables and figures. To investigate the effect of increasing the value of N on the approximate solution, consider a constant value for $M = 20$ and run the Matlab codes for different values of N and different values of fractional derivatives α and β, and report the obtained results in Table 4. Also, the error figures for $M = 20, N = 160$ and different values of α and β have been plotted in Figure 3. The effect of increasing M in approximate solution have been investigated in Table 5. From the reported results in Tables 4 and 5, it conclude that by increasing the values of M and N, and consequently decreasing the values of spatial step sizes in x and y directions, the values of maximum error are reduced and more accurate results are provided. Also, it follows that the computational convergence order is about 2. The behaviour of absolute error of described method for $u(0.5, 0.5, t)$ are depicted in Figure 4, where $0 \leq t \leq 1$ and $M = N = 10$ and $\alpha = \beta = 1.1, 1.2$ (left) and $\alpha = \beta = 1.9, 2$ (Right).

5   Conclusion

In this article, the Caputo fractional derivatives of order α and β are estimated via linear spline approximation, and then some finite difference formulas of order 2 are used to approximate the second-order derivatives with respect to x and y. Therefore, the solution of 2D stochastic space fractional telegraph equation is transformed into the solution of a system of IVPs with

Table 5: Numerical results of Example 4.2 with $N = 10$ at final time $T = 1$.

| M	$\alpha = \beta = 1.1$		$\alpha = \beta = 1.2$		$\alpha = \beta = 1.9$		$\alpha = \beta = 2$	
	L_∞-error	C_y-order	L_∞-error	C_y-order	L_∞-error	C_y-order	L_∞-error	C_y-order
10	6.5431×10^{-2}	——	4.0081×10^{-2}	——	1.2743×10^{-2}	——	8.0425×10^{-3}	——
20	1.6872×10^{-2}	1.9553	1.0254×10^{-2}	1.9667	3.1435×10^{-3}	2.0192	2.1486×10^{-3}	1.9042
40	3.9436×10^{-3}	2.0970	2.6437×10^{-3}	1.9555	7.9427×10^{-4}	1.9846	5.4612×10^{-4}	1.9761
80	9.8274×10^{-4}	2.0046	6.2412×10^{-4}	2.0826	1.8402×10^{-4}	2.1097	1.2937×10^{-4}	2.0777
160	2.3681×10^{-4}	2.0530	1.5437×10^{-4}	2.0154	4.5842×10^{-5}	2.0051	3.2702×10^{-5}	1.9840
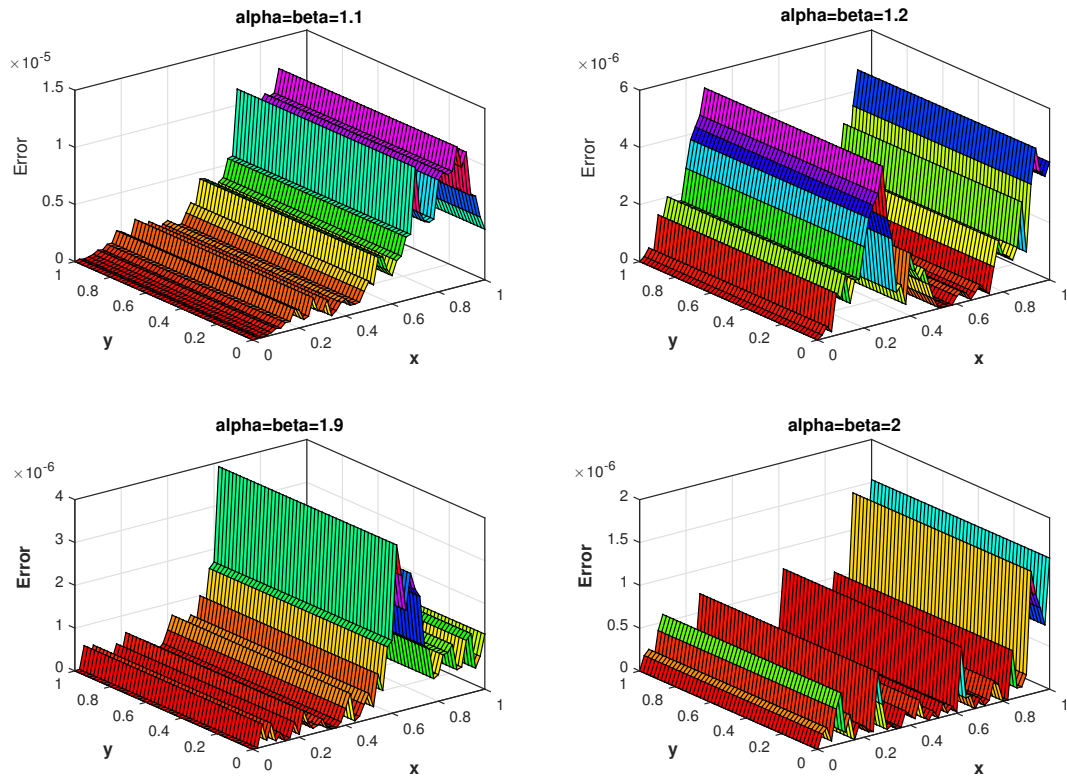
Figure 3: Absolute error of Example 4.2 for $M = 20, N = 160$ and different values of α and β at final time $T = 1$.

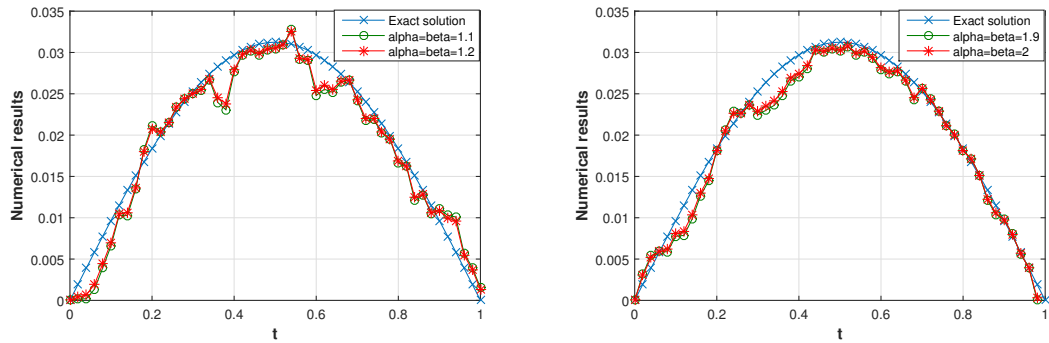Figure 4: Absolute error at $x = y = 0.5$ of Example 4.2 for different values of α and β with $M = N = 10$.

unknown error term $\overrightarrow{V} \simeq O(\Delta x^2 + \Delta y^2)$. By neglecting unknown error term $\overrightarrow{V}$ and using ODEs solver in Matlab software, the numerical solution is achieved. Although Matlab software is used to implement our programming codes, any other mathematical software with a library ODEs solver can be applied. The accuracy, efficiency and applicability of the mentioned method are checked via two test problems. In these examples, the effect of increasing M and N, or decreasing spatial step size Δx and Δy has been investigated. The numerical results reported in tables reveal that by increasing the number of mesh points in x and y directions, more accurate solution is obtained and the values of maximum error are reduced. Also, the influence of values of α and β in approximate solution have been tested and have been demonstrated that as α and β approach to 2, the values of maximum error is reduced.

Conflicts of Interest. The authors declare that they have no conflicts of interest regarding the publication of this article.

References

[1] M. Lakestani and B. N. Saray, Numerical solution of telegraph equation using interpolating scaling functions, *Comput. Math. Appl.* **60** (2010) 1964–1972, https://doi.org/10.1016/j.camwa.2010.07.030.

[2] P. M. Jordan and A. Puri, Digital signal propagation in dispersive media, *J. Appl. Phys.* **85** (1999) 1273–1282.

[3] V. H. Weston and S. He, Wave splitting of the telegraph equation in R3 and its application to inverse scattering, *Inverse Probl.* **9** (1993) #789, https://doi.org/10.1088/0266-5611/9/6/013.

[4] Y. H. Youssri and W. M. Abd-Elhameed, Numerical spectral Legendre-Galerkin algorithm for solving time fractional telegraph equation, *Rom. J. Phys.* **63** (2018) 1–16.

[5] O. Tasbozan and A. Esen, Quadratic B-spline Galerkin method for numerical solutions of fractional telegraph equations, *Bull. Math. Sci. Appl.* **18** (2017) 23–39.

[6] O. Tasbozan and A. Esen, Collocation solutions for the time fractional telegraph equation using cubic B-spline finite elements, *An. Univ. Vest Timiş. Ser. Mat.-Inform.* **57** (2019) 131–144, https://doi.org/10.2478/awutm-2019-0020.

[7] E. Shivanian, S. Abbasbandy and A. Khodayari, Numerical simulation of 1D linear telegraph equation with variable coefficients using meshless local radial point interpolation (MLRPI), *Int. J. Ind. Math.* **10** (2018) 151–164.

[8] A. H. Bhrawy, M. A. Zaky and J. A. T. Machado, Numerical solution of the two-sided space–time fractional telegraph equation via Chebyshev tau approximation, *J. Optim. Theory Appl.* **174** (2017) 321–341, https://doi.org/10.1007/s10957-016-0863-8.

[9] V. R. Hosseini, W. Chen and Z. Avazzadeh, Numerical solution of fractional telegraph equation by using radial basis functions, *Eng. Anal. Bound. Elem.* **38** (2014) 31–39, https://doi.org/10.1016/j.enganabound.2013.10.009.

[10] Ş. Yüzbaşı and M. Karaçayır, A Galerkin-like scheme to solve two-dimensional telegraph equation using collocation points in initial and boundary conditions, *Comput. Math. Appl.* **74** (2017) 3242–3249, https://doi.org/10.1016/j.camwa.2017.08.020.

[11] S. Singh, V. K. Patel, V. K. Singh and E. Tohidi, Application of Bernoulli matrix method for solving two-dimensional hyperbolic telegraph equations with Dirichlet boundary conditions, *Comput. Math. Appl.* **75** (2018) 2280–2294, https://doi.org/10.1016/j.camwa.2017.12.003.

[12] D. Rostamy, M. Emamjome and S. Abbasbandy, A meshless technique based on the pseudospectral radial basis functions method for solving the two-dimensional hyperbolic telegraph equation, *Eur. Phys. J. Plus.* **132** (2017) 1–11, https://doi.org/10.1140/epjp/i2017-11529-2.

[13] E. Shivanian, Spectral meshless radial point interpolation (SMRPI) method to two-dimensional fractional telegraph equation, *Math. Methods Appl. Sci.* **39** (2016) 1820–1835, https://doi.org/10.1002/mma.3604.

[14] N. Samadyar and F. Mirzaee, Numerical solution of two-dimensional weakly singular stochastic integral equations on non-rectangular domains via radial basis functions, *Eng. Anal. Bound. Elem.* **101** (2019) 27–36, https://doi.org/10.1016/j.enganabound.2018.12.008.

[15] M. H. Heydari, M. R. Hooshmandasl, F. M. Maalek Ghaini and C. Cattani, A computational method for solving stochastic Itô–Volterra integral equations based on stochastic operational matrix for generalized hat basis functions, *J. Comput. Phys.* **270** (2014) 402–415, https://doi.org/10.1016/j.jcp.2014.03.064.

[16] F. Mirzaee, S. Alipour and N. Samadyar, Numerical solution based on hybrid of block-pulse and parabolic functions for solving a system of nonlinear stochastic Itô–Volterra integral equations of fractional order, *J. Comput. Appl. Math.* **349** (2019) 157–171, https://doi.org/10.1016/j.cam.2018.09.040.

[17] F. Mirzaee and N. Samadyar, On the numerical solution of stochastic quadratic integral equations via operational matrix method, *Math. Methods Appl. Sci.* **41** (2018) 4465–4479, https://doi.org/10.1002/mma.4907.

[18] R. Zeghdane, Numerical solution of stochastic integral equations by using Bernoulli operational matrix, *Math. Comput. Simulation* **165** (2019) 238–254, https://doi.org/10.1016/j.matcom.2019.03.005.

[19] F. Mirzaee, N. Samadyar and S. F. Hoseini, Euler polynomial solutions of nonlinear stochastic Itô–Volterra integral equations, *J. Comput. Appl. Math.* **330** (2018) 574–585, https://doi.org/10.1016/j.cam.2017.09.005.

[20] M. Dehghan and M. Shirzadi, Numerical solution of stochastic elliptic partial differential equations using the meshless method of radial basis functions, *Eng. Anal. Bound. Elem.* **50** (2015) 291–303, https://doi.org/10.1016/j.enganabound.2014.08.013.

[21] A. Barth and T. Stüwe, Weak convergence of Galerkin approximations of stochastic partial differential equations driven by additive Lévy noise, *Math. Comput. Simul.* **143** (2018) 215–225, https://doi.org/10.1016/j.matcom.2017.03.007.

[22] M. Dehghan and M. Shirzadi, A meshless method based on the dual reciprocity method for one-dimensional stochastic partial differential equations, *Numer. Methods Partial Differential Equations* **32** (2016) 292–306, https://doi.org/10.1002/num.21995.

[23] M. Dehghan and M. Shirzadi, Meshless simulation of stochastic advection–diffusion equations based on radial basis functions, *Eng. Anal. Bound. Elem.* **53** (2015) 18–26, https://doi.org/10.1016/j.enganabound.2014.11.011.

[24] F. Mirzaee and N. Samadyar, Combination of finite difference method and meshless method based on radial basis functions to solve fractional stochastic advection–diffusion equations, *Eng. Comput.* **36** (2020) 1673–1686, https://doi.org/10.1007/s00366-019-00789-y.

[25] M. H. Heydari, M. R. Hooshmandasl, G. Barid Loghmani and C. Cattani, Wavelets Galerkin method for solving stochastic heat equation, *Int. J. Comput. Math.* **93** (2016) 1579–1596, https://doi.org/10.1080/00207160.2015.1067311.

[26] Y. Salehi, M. T. Darvishi and W. E. Schiesser, Numerical solution of space fractional diffusion equation by the method of lines and splines, *Appl. Math. Comput.* **336** (2018) 465–480, https://doi.org/10.1016/j.amc.2018.04.053.

[27] S. Kazem and M. Dehghan, Semi-analytical solution for time-fractional diffusion equation based on finite difference method of lines (MOL), *Eng. Comput.* **35** (2019) 229–241, https://doi.org/10.1007/s00366-018-0595-5.

[28] M. F. Causley, H. Cho, A. J. Christlieb and D. C. Seal, Method of lines transpose: high order L-stable $\mathcal{O}(N)$ schemes for parabolic equations using successive convolution, *SIAM J. Numer. Anal.* **54** (2016) 1635–1652, https://doi.org/10.1137/15M1035094.

[29] S. Hamdi, W. H. Enright, Y. Ouellet and W. E. Schiesser, Method of lines solutions of the extended Boussinesq equations, *J. Comput. Appl. Math.* **183** (2005) 327–342, https://doi.org/10.1016/j.cam.2004.12.036.

[30] P. Rahimkhani, Y. Ordokhani and P. M. Lima, An improved composite collocation method for distributed-order fractional differential equations based on fractional Chelyshkov wavelets, *Appl. Numer. Math.* **145** (2019) 1–27, https://doi.org/10.1016/j.apnum.2019.05.023.

[31] E. Keshavarz and Y. Ordokhani, A fast numerical algorithm based on the Taylor wavelets for solving the fractional integro-differential equations with weakly singular kernels, *Math. Methods Appl. Sci.* **42** (2019) 4427–4443, https://doi.org/10.1002/mma.5663.